



ELSEVIER

Nuclear Instruments and Methods in Physics Research A 441 (2000) 459–467

**NUCLEAR
INSTRUMENTS
& METHODS
IN PHYSICS
RESEARCH**
Section A

www.elsevier.nl/locate/nima

Measurement of material uniformity using 3-D position sensitive CdZnTe gamma-ray spectrometers

Z. He^{a,*}, W. Li^a, G.F. Knoll^a, D.K. Wehe^a, C.M. Stahle^b

^aDepartment of Nuclear Engineering and Radiological Sciences, University of Michigan, Ann Arbor, MI 48109, USA

^bDetector Systems Branch, NASA Goddard Space Flight Center, Code 553, Greenbelt, MD 20771, USA

Received 12 August 1999; accepted 12 August 1999

Abstract

We present results from two 1 cm³ CdZnTe gamma-ray spectrometers with full 3-D position sensitivity. To our knowledge, these are the first reported semiconductor spectrometers that provide independent spectral data for each of over 2000 volume elements. Energy resolutions of 1.5–1.6% FWHM and position resolutions of 0.7 × 0.7 × 0.5 mm were obtained at 662 keV gamma-ray energy from the central region of both detectors for single-pixel events. With the 3-D position sensing capability, variations in spectral response over the detector volume were recorded using a ¹³⁷Cs source. These measurements allow a study of full-energy peak efficiency, mean ionization energy and electron trapping as a function of 3-D position. The effects of material non-uniformity on detector spectroscopic performance are discussed. © 2000 Elsevier Science B.V. All rights reserved.

PACS: 07.85.Ne

Keywords: Gamma-ray spectrometers; Semiconductor; CdZnTe; Position sensitive gamma-ray detectors

1. Introduction

Since the single polarity charge sensing method was implemented on solid-state semiconductor gamma-ray detectors [1], and the depth sensing technique was employed [2], the spectroscopic performance of CdZnTe gamma-ray detectors has been improved dramatically compared with that obtained on conventional detectors using planar electrodes [3]. However, the best energy resolution of ~ 1.8% FWHM obtained at 662 keV gamma-

ray energy on a relatively large volume (1 cm³) device [3] is still much worse than that predicted by the limit set by charge carrier statistics (~ 0.2% FWHM assuming a Fano factor of 0.1). Although experimental studies [3] indicated that the gamma-ray spectroscopic performance can be further improved by reducing the difference between weighting potentials of the collecting and the non-collecting anodes, other factors such as the variation of ionization energy due to gradients in the Zn concentration, the variation of electron trapping, and the presence of material defects could also degrade detector performance. This work investigates the effects of some of these factors in CdZnTe detectors.

*Corresponding author. Fax: +1-734-763-4540.

E-mail address: hezhong@umich.edu (Z. He)

Two 3-D position sensitive gamma-ray spectrometers were fabricated using wide band-gap semiconductor CdZnTe which can be operated at room temperature [4]. The detectors are 1 cm^3 cubic CdZnTe crystals with 11×11 pixellated anodes. The lateral (x and y) position of gamma-ray interaction is obtained from the location of the pixel anode that collects electrons, and the depth (z) is obtained from the ratio of the cathode and the anode signals. Energy spectra from 662 keV incident gamma-rays were obtained for each of the ~ 2400 voxels in both of the two 1 cm^3 cube CdZnTe devices. After 3-D corrections for the non-uniformity of electron trapping of the detector material and for the gain variation of the readout circuitry, the measured energy resolution was 1.5% and 1.6% FWHM from combined output of the central 9×9 pixels on the first and the second detectors, respectively, for single-pixel events.

Some properties, such as current–voltage characteristics, thermally stimulated current, charge carrier mobilities and mean lifetimes, and the variation of Zn concentrations have been measured across the area of thin crystals by other groups [5,6]. However, with 3-D position sensitivity available for the first time in CdZnTe detectors, the variation of material characteristics throughout the detector volume which are directly related to the spectroscopic performance of the detector can now be observed with a spatial resolution of $0.7 \times 0.7 \times 0.5$ mm. These spatially-varying characteristics include: the gamma-ray detection efficiency, electron trapping and the average ionization energy of the CdZnTe material.

2. Data collection

Two discrimination grade CdZnTe crystals ($\#eV - 1404 - 10$ and $\#eV - 1404 - 11$) were used to construct the devices.¹ In order to avoid the ambiguity of gamma-ray interaction position of multiple-interaction events, only events which the electrons generated by a gamma-ray interaction are

collected on a single anode pixel were selected for obtaining energy spectra of each voxel. Monte-Carlo simulations (Fig. 3, Ref. [7]) show that the full-energy single-pixel events are dominated by photoelectric interactions in which all gamma-ray energy was deposited locally. The characteristics of the photopeaks (photopeak areas, FWHM and amplitude centroids) were recorded to show their relative variation as a function of 3-D position within the detector.

3. Variation of full-energy peak efficiency

To observe whether the full-energy peak efficiency is uniform through the detector volume, a ^{137}Cs source was located ~ 5 cm from the cathode surface. The energy spectra were simultaneously collected at each voxel corresponding to a volume of $\sim 0.7 \times 0.7 \times 0.5$ mm within each detector [8], and the photopeak areas were measured. The photopeak area is the number of events in which all gamma-ray energy is deposited locally within one voxel during the data collection time. Because the attenuation length of 662 keV gamma-rays in CdZnTe is about 2.3 cm based on our simulations using GEANT3,² more than twice the detector thickness of 1 cm, it is expected that 662 keV gamma-rays interact with the detector material at all depths with an exponential attenuation. The experiment provides a depth parameter for each gamma-ray event, which is the ratio of pulse amplitudes of the cathode and the pixel anode signals. This depth parameter is quite linear with the geometrical depth of gamma-ray interaction between the cathode and about 1 mm from the anode surface, but is non-linear in the immediate vicinities of both the cathode and the anode. Our measurements on the first detector ($\#1$) show that the variation of the photopeak area as a function of the depth parameter under each anode pixel is quite flat between the cathode and the anode, and has a pile-up peak near the cathode surface. An example of such a measurement under an anode pixel of detector $\#1$ is shown in Fig. 1.

¹eV Products, 375 Saxonburg Boulevard, Saxonburg, PA 16056, USA.

²GEANT3, CERN, Geneva, Switzerland.

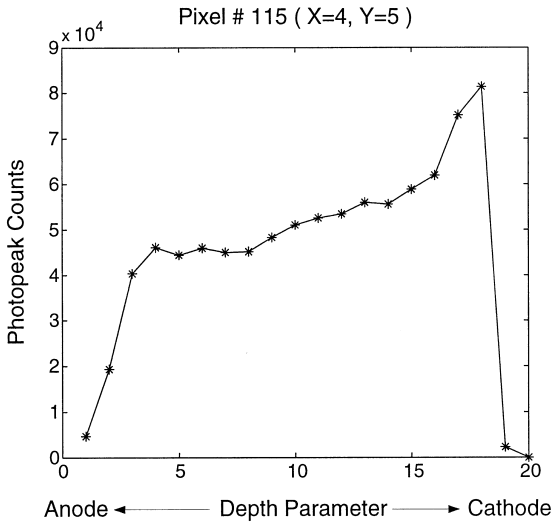


Fig. 1. Photopeak area as a function of gamma-ray interaction depth parameter under an anode pixel of detector #1.

However, when the photopeak area as a function of the depth parameter was obtained from the second detector (#2), significant variations were observed. We can loosely categorize the behavior of the full-energy peak efficiency under each anode pixel into three groups: (1) Normal pixels: there is no significant loss of efficiency between the cathode and the anode. An example is shown at the top of Fig. 2. (2) Pixels with defects located in the middle: there is severe loss of efficiency between the cathode and the anode, such as the example shown in the center of Fig. 2. Interestingly, the efficiency near both the cathode and the anode looks normal. Since these are relative measurements, the loss of full-energy peak efficiency must originate from the detector material, not from the readout electronic system. This indicates that some regions of the crystal produce significantly lower number of full-energy absorption events than other parts of the crystal. (3) Pixels with defects near the cathode side: there is severe loss of efficiency on the cathode side as shown at the bottom of Fig. 2. This loss could be caused by electron traps, such as a grain boundary which prevents a significant fraction of electrons from reaching the anode surface. Therefore, the event was not registered within the photopeak energy window.

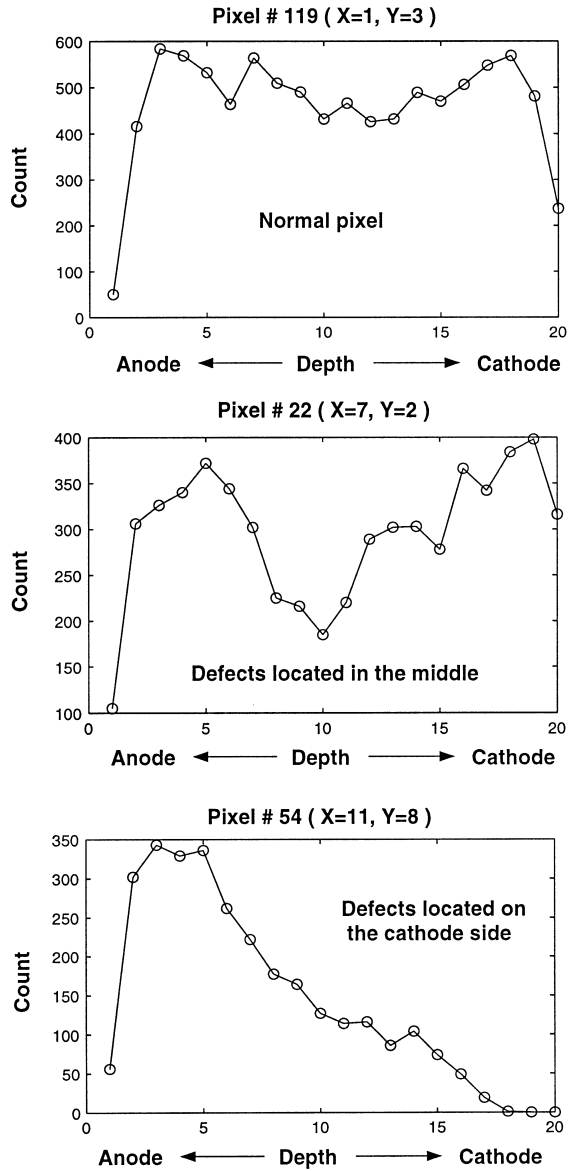


Fig. 2. Pixel categorized by the location of defects under each anode pixel (detector #2).

In order to display our observations, each anode pixel was classified according to one of the three categories defined above. Their lateral distribution is shown in Fig. 3. It is evident that each type tends to occupy a continuous region. This behavior supports the observation that the material defects are real and not from the result of readout error. In

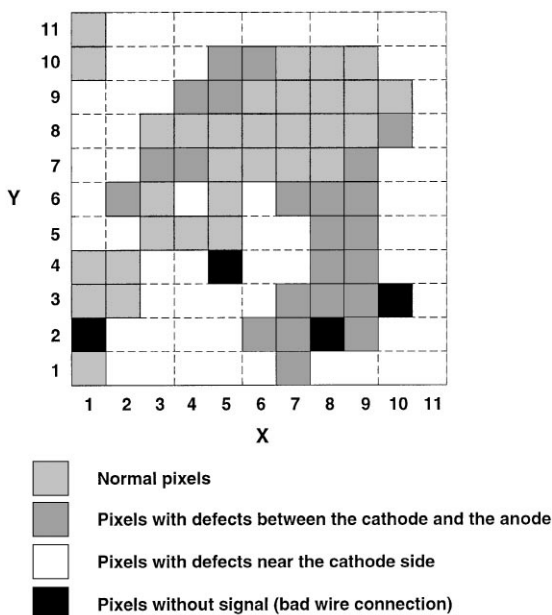


Fig. 3. The lateral location of each type of defect obtained from detector #2.

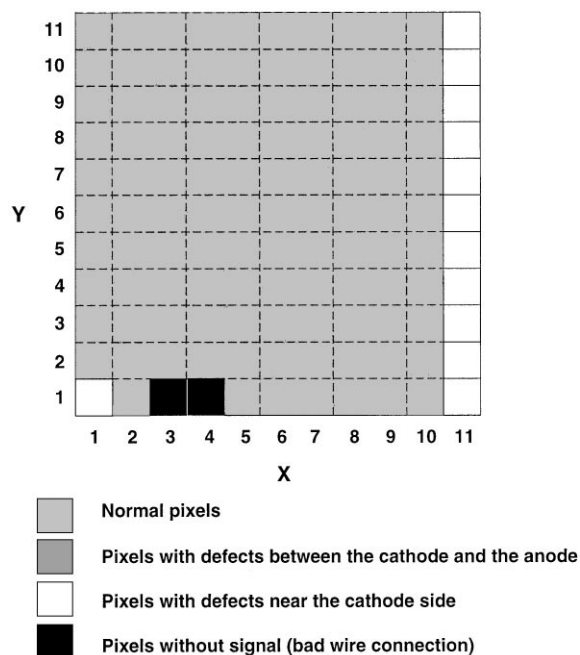


Fig. 4. The lateral location of each type of defect obtained from detector #1.

addition, the geometrical distribution shows the lateral scale of the defect structures.

In contrast, no defective region was observed within the central region of the first detector, except under a column of peripheral pixels and a corner pixel. The mapping of detection efficiency of detector #1 is shown in Fig. 4. It was observed that the full-energy peak efficiency also varies as a function of lateral location of anode pixels. Further investigation is needed.

4. Observation of electron traps

Although no significant loss of full-energy peak efficiency was observed in the central region of the first 3-D CdZnTe detector, significant degradation of energy resolution was recorded in some of its regions (the same phenomenon was seen in both detectors). Energy spectra of ¹³⁷Cs were obtained as a function of the depth parameter under each anode pixel, and the results from two typical pixels are shown in Figs. 5 and 6.

In Fig. 5, there is no abrupt change either in the photopeak area and in energy resolution when the interaction depth varies from the anode to the cathode surface. The results shown in Fig. 6, in contrast, show that even when no significant loss of efficiency was seen along the depth coordinate, the energy resolution becomes noticeably worse from certain depths between the anode and the cathode, and continuously deteriorates towards the cathode surface. There are two possibilities for the cause of this degradation of energy resolution. The first is that there is an region of enhanced electron trapping, such as a grain boundary, located at where the energy resolution starts to deteriorate. Its presence would degrade the energy resolution for those events for which electrons must pass through this region, i.e., when the interaction depth is between the trap and the cathode. The second possibility could be the variation of material properties in that region, such as the variation of Zn concentration within the crystal. Based on the results by Toney et al. [6], the change of 1–2% of pulse amplitude shown in our measurements (which broadens the

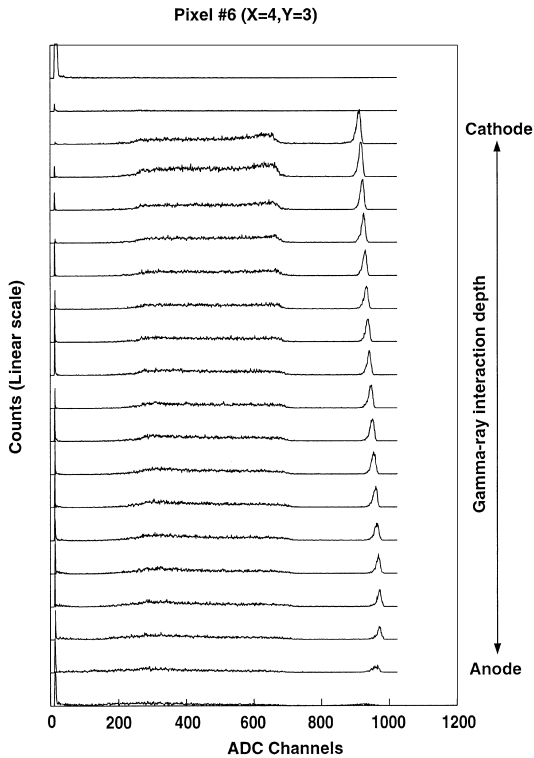


Fig. 5. The energy spectra (^{137}Cs) of single-pixel events obtained as a function of gamma-ray interaction depth from detector #1. No significant change of energy resolution is observed.

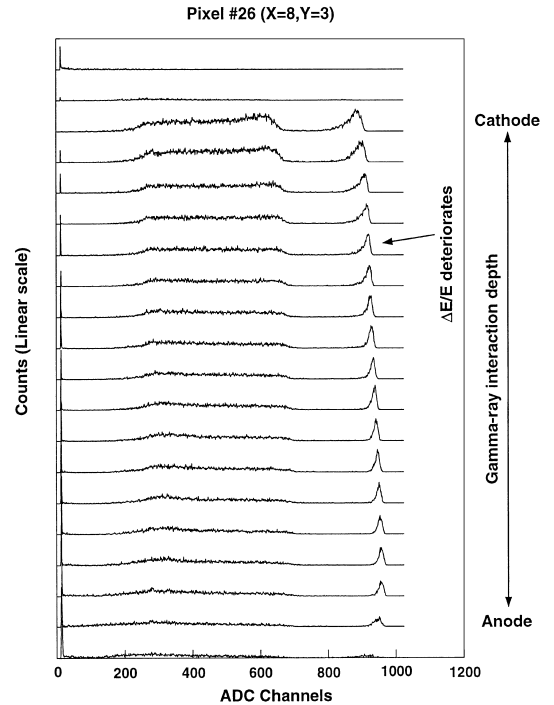


Fig. 6. The energy spectra (^{137}Cs) of single-pixel events obtained as a function of gamma-ray interaction depth from detector #1. The energy resolution degrades significantly when the depth parameter is greater than 14.

photopeak) requires a change of 2.6–5.2% in the Zn concentration. This is not likely to happen within the scale of $\sim \text{mm}$ (the dimension of one voxel) from previous measurements [6]. In addition, it has been observed that the energy resolution always deteriorates more severely at depths that are near to the cathode surface. This regularity is a strong evidence that counters the explanation that the energy degradation is linked to the variation of mean ionization energy of CdZnTe. It would be very unlikely that the fluctuation of mean ionization energy always increases towards the cathode side, since the relative orientation of the cathode was chosen randomly. From these observations, although the possibility of degradation of energy resolution caused by the fluctuation of mean ionization energy cannot be ruled out, it is more likely that the effect is caused by electron traps, such as grain boundaries, voids, Tl inclusions and twins,

located between the cathode and the anode that affect only a small fraction of transiting electrons.

5. Variation of electron trapping

Although the full-energy peak efficiency of detector #2 varies significantly within its volume, the amplitude of the photopeak centroid decreases smoothly from the anode to the cathode due to electron trapping. This indicates that the mean ionization energy does not change abruptly within the detector volume. An example is shown in Fig. 7. The sharp decrease corresponding to depth parameters less than 3 is from the non-linear region of the weighting potential in the vicinity of each anode pixel. It is evident from Fig. 7 that about 10% and 5% of the electrons are trapped through 1 cm thick CdZnTe at cathode biases of 1400 and 2400 V,

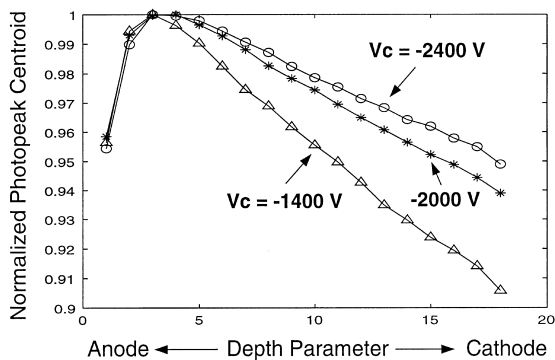


Fig. 7. The amplitude of the photopeak centroid versus the depth parameter measured at three cathode bias voltages. The data were collected from pixel #6 of detector #1 at 662 keV gamma-ray energy.

respectively. This behavior demonstrates that a good gamma-ray spectrometer using CdZnTe of this material quality must not only overcome the severe hole trapping problem, but must also be able to correct for electron trapping.

From measurements on the variation of the amplitude of photopeak centroid as a function of gamma-ray interaction depth, the mean $\mu_e \tau_e$ of detector material can be estimated under each anode pixel. This estimation is based on the following conditions: (1) The electron trapping follows the simple exponential relationship:

$$N(z) = N_0 \exp\left(-\frac{z}{\mu_e \tau_e E}\right) \quad (1)$$

where z is the electron drift distance, E is the electric field intensity and N is the number of free electrons at a drift distance of z . (2) The pulse amplitude obtained from each anode pixel is proportional to the number of electrons collected on the anode electrode. This simplified assumption ignores the variation of weighting potentials of each anode pixel within the linear region of the device. This underestimates the pulse amplitudes towards the anode side (N_0), and therefore tends to give a higher estimated $\mu_e \tau_e$ value. However, based on our calculations, this systematic error does not change our results significantly. (3) Photopeak events hav-

ing the largest depth parameter (highest cathode/anode ratio) are believed to come from the cathode surface, and those having the smallest depth parameter (lowest cathode/anode ratio) before the photopeak amplitude drops rapidly (the depth parameter = 3 in Fig. 7) are assumed to originate ~ 1 mm from the anode surface (about one anode pitch into the detector volume from the anode surface). For intermediate depth parameters that correspond to gamma-ray interactions between the cathode and 1 mm from the anode surface, the depth parameter is assumed to be linear with the geometrical depth and the measurement data is used for estimating the $\mu_e \tau_e$ values. Data collected in the vicinity of the anode surface (when the depth parameter is less than 3) were not used because the pulse amplitude is reduced severely in the non-linear region of the weighting potential.

The $\mu_e \tau_e$ values corresponding to the central 9×9 anode pixels were obtained using the linear least-squares method. To do so, the exponential relationship between $N(z)$ and z in Eq. (1) was converted to a linear relationship between $\ln N(z)$ and z as follows:

$$\ln\left(\frac{N(z)}{N_0}\right) = -\frac{z}{\mu_e \tau_e E}. \quad (2)$$

The slopes of the best linear fit provide values for $\mu_e \tau_e$. N_0 is the maximum value of the photopeak centroid (corresponding to that when the depth parameter = 3 in Fig. 7) and z is the electron drift distance from the location of the gamma-ray interaction to 1 mm from the anode surface.

The estimated values of $\mu_e \tau_e$ were confirmed by measurements at three different cathode biases (-1400 , -2000 and -2400 V), and the results are consistent. For example, the values of $\mu_e \tau_e$ obtained from anode pixel #6 of detector #1 are 5.8 , 6.1 and $6.1 \times 10^{-3} \text{ cm}^2/\text{V}$ at cathode biases of -1400 , -2000 and -2400 V, respectively. The small discrepancy between these values is probably due to systematic errors, such as the variation of weighting potentials within the linear region of the detector or the uncertainty in the calibration between the depth parameter and the geometrical depth. Since we divided the depth parameter

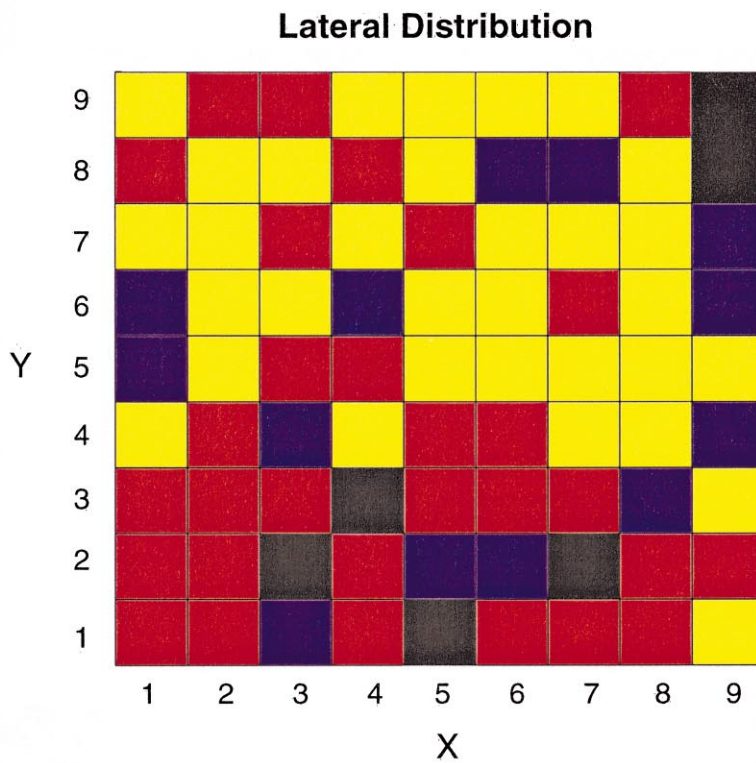
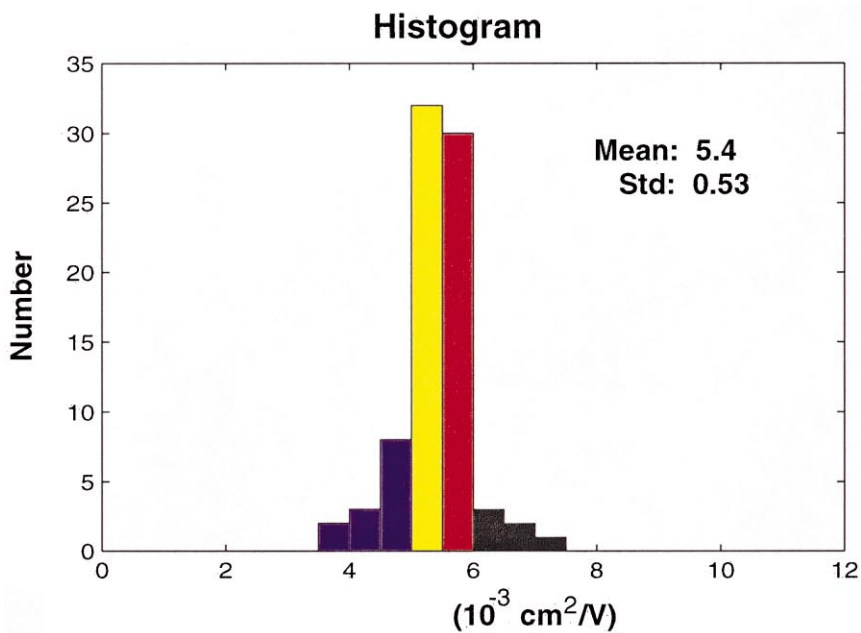


Fig. 8. Top: distribution of measured $\mu_c \tau_c$ values and their standard deviation obtained from detector #1. Bottom: lateral distribution of $\mu_c \tau_c$ values from the same detector.

equally into ~ 20 bins, it is expected that the depth parameter could change by up to $\frac{1}{20}$ (5%) between measurements at different biases. This would result in a change of up to 5% in the estimated values of $\mu_e\tau_e$ following from the linear relationship between $\mu_e\tau_e$ and z in Eq. (2).

The measured $\mu_e\tau_e$ values obtained from the central 9×9 anode pixels of detector #1 are summarized in Fig. 8. The mean $\mu_e\tau_e$ value and its standard deviation are $5.4 \pm 0.5 \times 10^{-3} \text{ cm}^2/\text{V}$. The lateral distribution of $\mu_e\tau_e$ values, as shown in the bottom of Fig. 8, shows no systematic correlation with location.

A similar result was obtained from the second detector. Since about $\frac{1}{3}$ of the volume in detector #2 has severe material defects (loss of full-energy peak efficiency), the $\mu_e\tau_e$ values cannot be obtained from some of the pixels. Especially when the defects are located on the cathode side, no depth calibration can be obtained from the cathode surface (corresponding to the maximum depth parameter). However, based on the results obtained from good anode pixels, under which no severe loss of efficiency was observed, values measured for $\mu_e\tau_e$ were quite similar to those from the first detector.

6. Summary

Some performance characteristics directly related to gamma-ray spectroscopy have been measured for the first time as a function of 3-D position within two 1 cm^3 cubic CdZnTe crystals. These include full-energy peak efficiency, the presence of electron traps, mean ionization energy, mean $\mu_e\tau_e$ values and their fluctuation. These measurements are made possible only with the newly available 3-D position sensitive CdZnTe gamma-ray spectrometers.

Severe loss of full-energy peak efficiency was observed in regions of one of the two detectors, but no significant loss of photopeak amplitude was seen. The effects of electron traps were observed and the locations of these traps can be identified with an accuracy of one voxel dimensions ($\sim 1 \times 1 \times 0.5 \text{ mm}$). The variation with lateral position of the mean electron $\mu_e\tau_e$ (underneath

each anode pixel) was measured. The observed fluctuation (standard deviation) in $\mu_e\tau_e$ is about 10%. Since the typical losses of electrons from the mid-point of the detector have absolute values of 2.5–5% at biases of 2400–1400 V between the cathode and the anode, the fluctuations in electron loss will be about 0.25–0.5% (standard deviation). Because $\text{FWHM} = 2.35\sigma$, this gives an estimation of 0.6–1.2% FWHM caused by the variation of electron trapping within the detector. This estimate shows that 3-D position sensing is necessary if better than 1% FWHM energy resolution is desired from our CdZnTe detectors. The material of detector #1 represents a quality typical of today's commercially available CdZnTe crystals.

Although the readout electronic system is complex, 3-D position sensitive semiconductor gamma-ray detectors offer great advantages in many imaging applications. In addition, they could achieve much lower noise level than other types of detectors because the leakage current through the bulk is shared by an array of anodes and the capacitance of each anode pixel is very small. If material non-uniformity of room temperature semiconductors, such as CdZnTe and HgI_2 , remains a limiting factor in detector performance, the best energy resolution can only be achieved by employing 3-D position sensitive detectors. Effects due to the non-uniformity of detector material can be corrected to the scale of one voxel in such a detector. Furthermore, when there are defects within the detector volume, such as inactive detection volume or electron traps, a 3-D position sensitive detector can identify the defect locations and allows the selection of detector volume for optimum gamma-ray spectroscopy.

Acknowledgements

This work was supported under DOE Grant DE-FG08-98NV13357. We thank N.A. Blum, J.S. Lehtonen and R.P. Aylor of Johns Hopkins University Applied Physics Laboratory for their work on the wire bonds and detector assembly, and James Berry for his technical assistance.

References

- [1] P.N. Luke, Appl. Phys. Lett. 65 (22) (1994) 2884.
- [2] Z. He et al., Nucl. Instr. and Meth. A 380 (1996) 228.
- [3] Z. He et al., Nucl. Instr. and Meth. A 388 (1997) 180.
- [4] Z. He et al., Nucl. Instr. and Meth. A 422 (1998) 180.
- [5] L. Verger et al., Nucl. Instr. and Meth. A 380 (1996) 121.
- [6] J.E. Toney et al., Nucl. Instr. and Meth. A 380 (1996) 132.
- [7] Y.F. Du et al., IEEE Transactions on Nuclear Science, Vol. 46(4) (1999) 844–847.
- [8] W. Li et al., IEEE Transactions on Nuclear Science, Vol. 46(3) (1999) 187–192.